European Journal of Radiology Open 8 (2021) 100374

Contents lists available at ScienceDirect

European Journal of Radiology Open

journal homepage: www.elsevier.com/locate/ejro

Multi-band whole-body diffusion-weighted imaging with inversion recovery fat saturation: Effects of respiratory compensation

Solveig Kärk Abildtrup Larsen *, Kim Sivesgaard, Erik Morre Pedersen

Department of Radiology, Aarhus University Hospital, Denmark

HIGHLIGHTS

- MB reduces DWIBS scan time which can be reinvested in respiratory compensation.
- MB enables respiratory trigger in DWIBS while maintaining low acquisition time.
- MB enables very fast DWIBS sequences that still produce acceptable image quality.

ARTICLE INFO

Keywords:
Diffusion magnetic resonance imaging
Multi-band
Respiratory compensation
Testicular neoplasm

ABSTRACT

Purpose: To prospectively compare artefacts and image quality in testicular stage I cancer patients using different combinations of breathing schemes and Multi-band (MB) in whole-body DWIBS at 1.5 T.

Diffusion-Weighted whole-body Imaging with Background body signal Suppression (DWIBS) using inversion recovery (IR) fat saturation is a cornerstone in oncologic whole-body MRI, but implementation is restrained by long acquisition times. The new Multi-Band (MB) technique reduces scan time which can be reinvested in respiratory compensation.

Methods: Thirty testicular cancer stage I patients were included. Three variations of whole-body DWIBS were tested: Standard free Breathing (FB)-DWIBS, FB-MB-DWIBS and Respiratory triggered (RT)-MB-DWIBS. Artefacts and image quality of b = 800 s/mm^2 images were evaluated using a Likert scale. No pathology was revealed. SNR was calculated in a healthy volunteer.

Results: RT-MB-DWIBS was rated significantly better than FB-DWIBS in the thorax ($p < 0.001$) and abdomen ($p < 0.001$), but not in the pelvis ($p = 0.569$). FB-MB-DWIBS was ranked significantly lower than both FB-DWIBS ($p < 0.001$) and RT-MB-DWIBS ($p < 0.001$) at all locations. However, FB-MB-DWIBS was scanned in half the time without being less than "satisfactory". Few artefacts were encountered. SNR was similar for low-intensity tissues, but the SNR in high-intensity and respiratory-prone tissue (spleen) was slightly lower for FB-DWIBS than the other sequences.

Conclusion: Images produced by the sequences were similar. MB enables the use of respiratory trigger or can be used to produce very fast free-breathing DWI with acceptable image quality.

1. Introduction

Diffusion-weighted whole-body imaging with background body signal suppression (DWIBS) [1] is a diffusion weighted imaging (DWI) technique with inversion recovery (IR) fat saturation. IR fat saturation is currently the only fat saturation technique that reliably and reproducibly provides homogenous fat saturation across the entire body with DWI techniques [2,3]. DWIBS is being used in treatment response

Abbreviations: ADC, apparent diffusion coefficient; CT, computed tomography; DWI, diffusion-weighted imaging; DWIBS, diffusion-weighted whole-body imaging with background body signal suppression; EPI, echo planar imaging; FB, free-breathing; IR, inversion recovery; MB, multi-band; MRI, magnetic resonance imaging; NSA, number of signal averages; Pet, positron emission tomography; RF, radio frequency; ROI, region of interest; RT, respiratory triggered; SAR, specific absorption rate; SMS, simultaneous multislice; SNR, signal-to-noise ratio; SPAIR, spectral attenuated inversion recovery; T, tesla; TE, echo time; TR, repetition time; WB, whole-body.

* Corresponding author at: Department of Radiology, Aarhus University Hospital, Palle Juul-Jensens Boulevard 99, C118, 8200 Aarhus N, Denmark.
E-mail address: solveig.larsen@auh.rm.dk (S.K.A. Larsen).

https://doi.org/10.1016/j.ejro.2021.100374
Received 27 June 2021; Received in revised form 20 August 2021; Accepted 22 August 2021
Available online 26 August 2021

Table 1
MRI imaging parameters at 1.5 T.

	FB-DWIBS	FB-MB-DWIBS	RT-MB-DWIBS
Imaging mode	EPI SE single-shot	EPI SE single-shot	EPI SE single-shot
Acquired pixel size (mm)	4 × 4	4 × 4	4 × 4
Slice thickness (mm)	6	6	6
Plane	Axial	Axial	Axial
Stations	Thorax Abdomen Pelvis	Thorax Abdomen Pelvis	Thorax Abdomen Pelvis
TE (ms)	68	72	70
TR (ms)/scantime per resp. cycle	6531	3437	1774*/1 respiratory cycle
B-values (s/mm^2)	0, 50, 800	0, 50, 800	0, 50, 800
Number of signal averages	2, 2, 4	2, 2, 4	2, 2, 4
Fat suppression	STIR	STIR	STIR
SENSE factor	2	2	2
Multi-Band	No	Yes	Yes
Acceleration factor	–	2	2
Respiration	Free-breathing	Free-breathing	Respiratory trigger
Acquisition time per station (min)	2.17	1.12	2.06*

* Assuming a respiratory frequency of 20 per min / TR of 3000 ms.

assessment in several bone-metastasizing cancers and for assessment of multiple myeloma [4].

DWIBS is time consuming for large scan areas. Thus, the widespread implementation of whole-body DWI is restrained by long acquisition times. In addition to higher costs, a long acquisition time may impair patient cooperation, especially in frail patients or in patients experiencing pain or claustrophobia [5,6].

Acceleration techniques for acquisition of multiple slices at the same time such as Multi-Band (MB) or Simultaneous multislice (SMS) can reduce the acquisition time of DWI with 50 % or more (acceleration factor of 2 or higher) through simultaneous excitation and acquisition of multiple slices [6]. Acquisition of multiple slices and the subsequent image separation can be performed by several different techniques. MB is a SENSE approach, whereas other SMS techniques can be GRAPPA-based [7].

MB or SMS can be used to reduce scan time and thus decrease motion related problems due to long scan times and increase patient throughput in the MRI scanner. Alternatively, the time saved can be reinvested in respiratory compensation, increased coverage or increased resolution [6,8,9].

Previous studies outside the brain e.g. [8,10–14]) have all applied SMS to DWI with SPAIR fat saturation. In addition, most studies have focused either on single organs or regions and have been performed mainly at 3 T [16]. However, 1.5 T seems better suited than 3 T for IR fat saturation as the adiabatic IR fat saturation pulse is slice selective and needs to be adapted for MB. This poses additional challenges at 3 T because of SAR and RF power limitations impacting the bandwidth of the pulse required to realize decent fat suppression.

In movement-prone areas of the body, e.g., the upper abdomen, different schemes for respiratory compensation can be applied to DWI in an effort to increase image quality [9,15]. Compared to standard free-breathing using multiple acquisitions to reduce breathing artefacts, the use of respiratory trigger, navigator or breath-hold techniques will rapidly increase the acquisition time for the total examination. However, when SMS or MB is used in combination with

respiratory compensation, the acquisition time can potentially be reduced to a level realistic for clinical use, as the average length of a respiration (12–20/min, 3000−5000 ms/respiration [16]) compares well with an acceptable TR of the DWI sequence. Several studies have investigated different breathing schemes in DWI with SMS, but they have all focused on single organs and have all used SPAIR as opposed to IR fat saturation [9,12,17–19].

We hypothesized that reinvesting scan time gained by applying MB to respiratory triggering could improve whole-body DWIBS in areas with motion. In this prospective study of the first application of MB and respiratory trigger in whole-body DWIBS, we focus on investigating the quality of the b = 800 s/mm^2 images. The b = 800 s/mm^2 images are not intended to stand alone in clinical practice but are more prone to a potential SNR penalty and therefore relevant as the primary marker of image quality.

1.1. Aim

The aim of this study was to prospectively compare image quality and SNR for b = 800 s/mm^2 images in whole-body DWIBS at 1.5 T in a healthy male patient cohort in a healthy volunteer using three different combinations of breathing schemes and MB: standard free-breathing DWIBS (FB-DWIBS), free-breathing DWIBS with MB (FB-MB-DWIBS) and respiratory-triggered DWIBS with MB (RT-MB-DWIBS).

2. Materials and methods

2.1. Patients

From March to August 2018, 30 consecutive patients were included. The patients were scheduled for MRI of the retroperitoneum and pelvis as follow-up for testicular cancer stage I. In general, these patients are young, healthy males with no or little comorbidity. After orchiectomy, the patients are managed with watchful waiting without radiotherapy or chemotherapy [20]. At our institution, MRI including DWIBS is standard of care for these patients.

All procedures performed were in accordance with the ethical standards of the local ethics committee and with the 1964 Declaration of Helsinki and its later amendments or comparable ethical standards. The project was categorized as method development by the local ethics committee which waived the need for written informed consent. Despite this, all patients gave oral consent to additional MRI sequences being scanned and stored in anonymous form.

2.2. MRI protocol

The examinations were performed on a 1.5 T MRI scanner (Ingenia, release 5.3 software with DDAS spectrometer, Philips Medical Systems, Best, The Netherlands). The built-in posterior coil, dS head-neck coil and flex coverage anterior coil from the scanner vendor were used. A research-implementation of MB for DWIBS (Multiband for DWIBS patch release 2.0 on release 5.3 software, Philips) was used.

The research sequences were scanned in addition to the scheduled MRI protocol. The DWIBS sequence was scanned with three different combinations of breathing schemes and MB: standard free-breathing DWIBS (FB-DWIBS), free-breathing DWIBS with MB (FB-MB-DWIBS) and respiratory-triggered DWIBS with MB (RT-MB-DWIBS). Each sequence was scanned in three stations with coverage from the groin to approx. the neck.

The FB-DWIBS parameters were single-shot, echo-planar imaging sequence with IR fat saturation (inversion time (TI) = 180 ms), TR 6531 ms, TE 68 ms, 6 mm slices, 4 × 4 mm pixels, b-values (b = 0 s/mm^2 (2 NSA), b = 50 s/mm^2 (2 NSA), b = 800 s/mm^2 (4 NSA). FB-MB-DWIBS used the same scan parameters as FB-DWIBS with the addition of MB with acceleration factor 2 (resulting in halving of TR to 3437 ms and a slight increase of TE to 72 ms). RT-MB-DWIBS used the scan parameters of FB-MB-DWIBS with the addition of respiratory triggering (TR of 1 respiratory cycle with 1774 ms acquisition time per breath hold). For details, see Table 1.

The sequences included three b-values in preparation for future applications and generations of ADC-maps.

The acquisition time of the free-breathing sequences were 2.17 min

Table 2
SNR of b = 800 s/mm^2 images in a healthy volunteer.

	ROI area cm^2	Slices	ROI area total cm^2	SNR mean		
				FB-DWIBS	FB-MB-DWIBS	RT-MB-DWIBS
Spleen	2	16	32	16.9	13.7	16.2
Liver	15	19	285	3.9	3.3	3.5
Gluteal muscle	15	14	420	3.4	3.3	3.4

(FB-DWIBS) and 1.12 min (FB-MB-DWIBS). The acquisition time of the respiratory triggered sequence (RT-MB-DWIBS) depended on respiratory frequency, but was estimated to 2.06 min based on a respiratory frequency of 20/min. The true acquisition time was approx. 2−5 min.

In total, approx. 16 min scan time was used for the three whole-body DWI sequences.

The three DWIBS sequences were anonymized using Osirix Dicom Viewer software (version 10.0, Pixmeo, Bernex, Switzerland).

2.3. In vivo SNR analysis

In vivo analysis of SNR was performed in a healthy volunteer (34 years old). Two identical image sets were obtained for each DWIBS sequence. SNR was calculated by the difference method described for parallel imaging by Reeder et al. [21]. SNR was calculated in three tissues: the spleen, the liver and the gluteal muscles.

The spleen as a surrogate for high DWI intensity lesions as seen in relapse of TC in the retroperitoneal lymph nodes [20]. In addition, the spleen is prone to respiratory motion. A 2 cm^2 ROI (region of interest) was placed within the spleen in 16 slices on each DWIBS sequence. Thus, the SNR in the spleen was derived from a total of 32 cm^2 (approx. 200 voxels) in each sequence.

Two tissues with homogenous low DWI intensity were chosen: one prone to respiratory motion (the liver) and one without respiratory motion (the gluteal muscles). A 15 cm^2 ROI was placed in the liver (19 slices) and in both muscles (14 slices) on each DWIBS sequence. Thus, the SNR in each sequence was derived from a total of 285 cm^2 (approx. 1,700 voxels) in the liver and 420 cm^2 (approx. 2,600 voxels) in gluteal

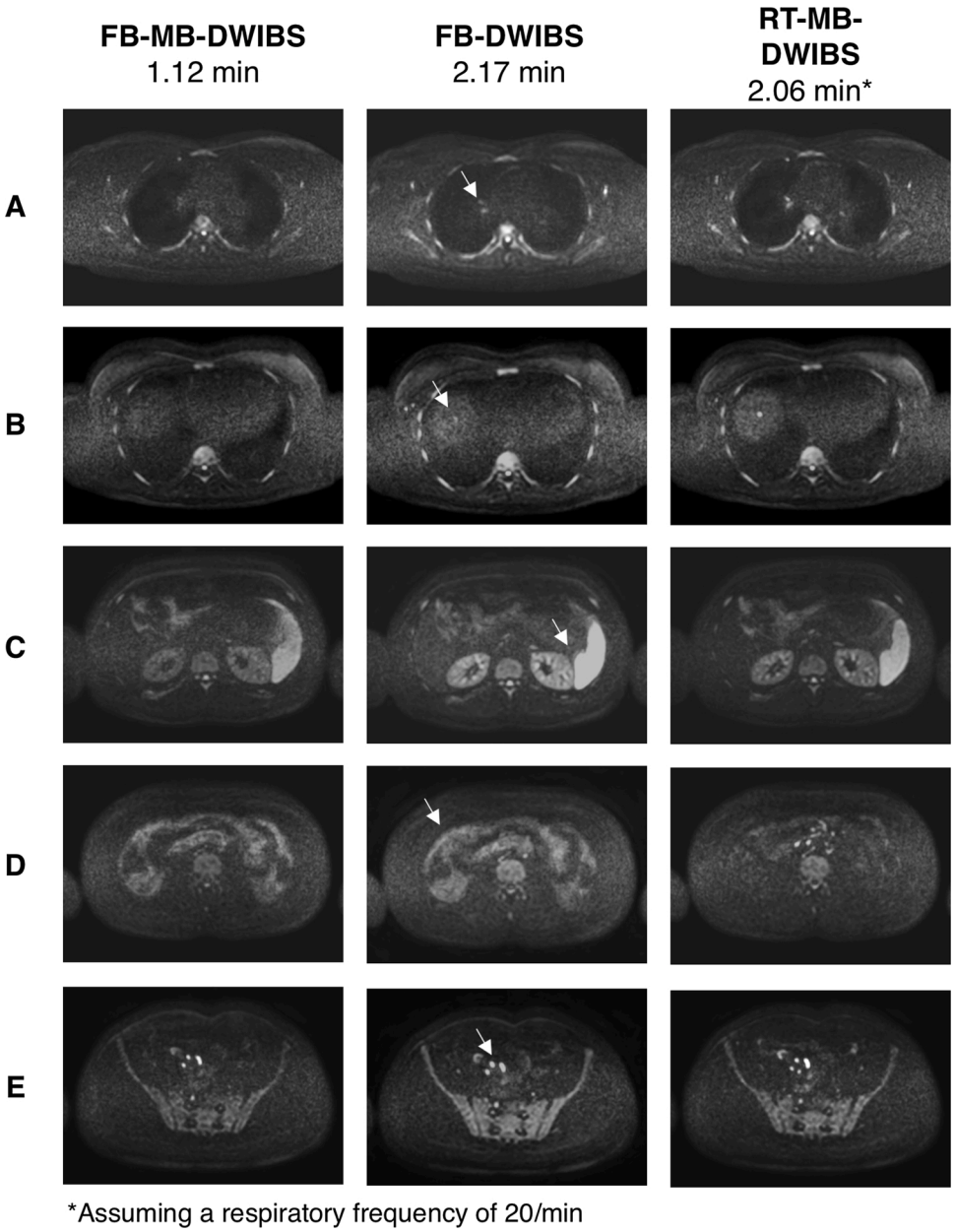

Fig. 1. Image examples. Corresponding slices of b800 s/mm^2 images from FB-DWIBS (standard), FB-MB-DWIBS and RT-MB-DWIBS in a 29-year old male.
A: Mediastinum: Notice the difference in lymph node visibility.
B: Upper abdomen: Notice the benign liver lesion with high signal intensity clearly visible on RT-MB-DWIBS, barely visible on FB-DWIBS and invisible on FB-MB-DWIBS.
C: Kidney and spleen: Notice the difference in spleen homogeneity and delineation.
D: Abdomen: Notice the difference in signal intensity from intraabdominal fat and intestines.
E: Pelvis: Notice the similarity in lymph node visibility.

Table 3
Artefacts with 95 % confidence intervals, Friedman test and Wilcoxon signed rank test. Modified Likert scale from 1 (high impact) to 5 (no impact). A p-value < 0.05 was considered statistically significant: * FB-DWIBS vs. FB-MB-DWIBS, ** FB-DWIBS vs. RT-MB-DWIBS, *** FB-MB-DWIBS vs. RT-MB-DWIBS.

	Station	FB-DWIBS	FB-MB-DWIBS	RT-MB-DWIBS	Friedman test (k3, n30)		Wilcoxon signed rank test P-value		
					Ft	p-value	*	**	***
Distortion	Thorax	4.9 (4.8–5.0)	4.6 (4.5–4.8)	4.4 (4.3–4.7)	6.45	< 0.05	< 0.05	< 0.001	0.063
	Abdomen	5.0 (-)	5.0 (-)	5.0 (-)	0.00	1.00	1.00	1.00	1.00
	Pelvis	4.9 (4.7–5.0)	4.9 (4.7–5.0)	4.9 (4.7–5.0)	0.00	1.00	1.00	1.00	1.00
	Average	4.9 (4.9–5.0)	4.8 (4.8–4.9)	4.8 (4.7–4.9)	3.20	0.20	< 0.05	< 0.001	0.063
Ghosting	Thorax	5.0 (-)	5.0 (-)	5.0 (-)	0.00	1.00	1.00	1.00	1.00
	Abdomen	5.0 (-)	5.0 (-)	5.0 (-)	0.00	1.00	1.00	1.00	1.00
	Pelvis	5.0 (-)	5.0 (-)	5.0 (-)	0.00	1.00	1.00	1.00	1.00
	Average	5.0 (-)	5.0 (-)	5.0 (-)	0.00	1.00	1.00	1.00	1.00
Fat saturation artefacts	Thorax	5.0 (-)	4.8 (4.7–5.0)	5.0 (4.9–5.0)	1.05	0.59	0.063	1.00	0.13
	Abdomen	4.9 (4.7–5.90)	4.4 (4.2–4.7)	4.8 (4.7–5.0)	7.35	< 0.05	< 0.001	0.50	< 0.001
	Pelvis	4.9 (4.8–5.0)	4.6 (4.4–4.9)	4.9 (4.8–5.0)	3.22	0.20	< 0.05	1.00	< 0.05
	Average	4.9 (4.9–5.0)	4.6 (4.5–4.8)	4.9 (4.8–5.0)	7.27	< 0.05	< 0.001	0.50	< 0.05
Motion artefacts	Thorax	5.0 (-)	5.0 (-)	5.0 (-)	0.00	1.00	1.00	1.00	1.00
	Abdomen	4.4 (4.3–4.6)	4.4 (4.2–4.6)	4.4 (4.1–4.6)	0.15	0.93	1.00	0.50	1.00
	Pelvis	4.7 (4.5–4.9)	4.7 (4.5–4.9)	4.7 (4.5–4.8)	0.05	0.98	1.00	1.00	1.00
	Average	4.7 (4.6–4.8)	4.7 (4.6–4.8)	4.7 (4.6–4.8)	0.20	0.90	0.50	0.50	1.00
Metal artefacts	Thorax	4.8 (4.7–5.0)	4.8 (4.7–5.0)	4.8 (4.7–5.0)	0.00	1.00	1.00	1.00	1.00
	Abdomen	5.0 (4.8–5.1)	5.0 (4.8–5.1)	5.0 (4.8–5.1)	0.15	0.93	1.00	1.00	1.00
	Pelvis	4.9 (4.8–5.0)	4.9 (4.8–5.0)	4.9 (4.8–5.0)	0.05	0.98	1.00	1.00	1.00
	Average	4.9 (4.8–5.0)	4.9 (4.8–4.9)	4.9 (4.8–4.9)	0.20	0.90	1.00	1.00	1.00

muscles.

2.4. Image quality analysis

Assessment of b = 800 s/mm^2 image quality was performed by two radiologists with four and ten years of experience in whole-body DWIBS using Osirix. The three sequences were viewed simultaneously side-by-side, but the readers were blinded with regards to breathing scheme and the use of MB. The sequences were evaluated in three stations: thorax, abdomen and pelvis.

First, artefacts were evaluated in consensus as either distortion, ghosting, fat saturation artefacts, motion artefacts or metal artefacts. The impact of artefacts on diagnostic validity was evaluated using a modified Likert scale from 1 (high impact) to 5 (no impact).

Second, subjective image quality was evaluated independently by each reader. The sequences were ranked: 1 (worst), 2 (intermediate) or 3 (best). Two sequences could not be given the same rank. The image quality was evaluated using a modified Likert scale: 1 (unacceptable), 2 (poor), 3 (satisfactory), 4 (good) or 5 (excellent). Excellent was defined as the best possible quality for whole-body DWIBS. The following parameters of image quality were evaluated: overall region quality, overall region sharpness, detection of lymph nodes, contrast of mediastinum vs. lung, medulla, spleen homogeneity, liver delineation and prostate delineation.

Assessment data were collected and managed using the REDCap electronic data capture tool.

2.5. Statistical analysis

Statistical analysis was performed using STATA 16.1 (STATA Corp, Texas, USA). Average values and 95 % confidence intervals were calculated. Likert scores and ranks were compared using Friedman test followed by Wilcoxon signed-rank test for paired non-parametric data [22] in three sets: FB-DWIBS vs. FB-MB-DWIBS, FB-DWIBS vs. RT-MB-DWIBS and FB-MB-DWIBS vs. RT-MB-DWIBS. A p-value <0.05 was considered statistically significant.

Interobserver agreement was measured by calculating linear weighted kappa for multiple categories. The strength of agreement was defined as: <0 (poor), 0.00–0.20 (slight), 0.21–0.40 (fair), 0.41–0.60 (moderate), 0.61–0.80 (substantial) and 0.81–1.00 (almost perfect) [23].

3. Results

3.1. In vivo SNR analysis

In the high-intensity and respiratory-prone tissue of the spleen, the mean SNR was 16.9 for FB-DWIBS, 16.2 for RT-MB-DWIBS and 13.7, for FB-MB-DWIBS. In the low-intensity, respiratory-prone liver tissue, the mean SNR was 3.9 for FB-DWIBS, 3.5 for RT-MB-DWIBS and 3.3 for FB-MB-DWIBS. In the low-intensity, non-moving tissue of the gluteal muscles, the mean SNR was 3.4 for FB-DWIBS, 3.4 for RT-MB-DWIBS and 3.3 for FB-MB-DWIBS (Table 2).

3.2. Patients

Patient median age was 34 years [range 22–61 years]. The clinical part of all 30 MRI scans were normal without pathology. DWIBS image examples can be found in Fig. 1.

3.3. Artefacts

Average scores of artefacts incl. 95 % confidence intervals and p-values are listed in Table 3 and Figs. 2 and 3. Image examples in Fig. 4.

Overall, very few images were impacted by artefacts. Motion artefacts were not present in the thorax, distortion was not present in the abdomen and ghosting was not present at all.

In the thorax, FB-DWIBS was significantly less impacted by distortion than both FB-MB-DWIBS ($p < 0.05$) and RT-MB-DWIBS ($p < 0.001$). In the abdomen and pelvis, FB-MB-DWIBS was significantly more impacted by fat saturation artefacts than both FB-DWIBS (both $p < 0.001$) and RT-MB-DWIBS (both $p < 0.05$). All other differences were non-significant (Table 4).

3.4. Subjective image parameters

Average ranking scores incl. 95 % confidence intervals and p-values are listed in Table 3. RT-MB-DWIBS was rated significantly higher than FB-DWIBS in both thorax and abdomen (both $p < 0.001$), but not in the pelvis ($p = 0.57$). FB-MB-DWIBS was ranked significantly lower than both FB-DWIBS (all $p < 0.001$) and RT-MB-DWIBS (all $p < 0.001$).

Average scores of artefacts incl. 95 % confidence intervals and p-values are listed in Table 5 and Figs. 2 and 3. All three sequences scored near maximum for medulla signal quality (all average scores >4.9, p-

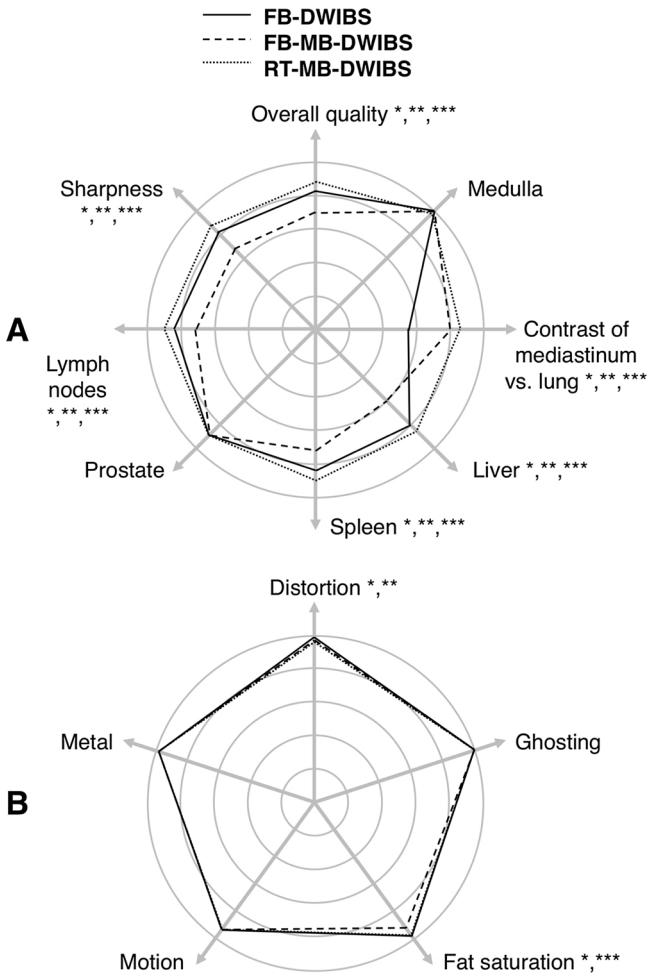

Fig. 2. Subjective image quality and artefacts. A p-value < 0.05 was considered statistically significant: * FB-DWIBS vs. FB-MB-DWIBS, ** FB-DWIBS vs. RT-MB-DWIBS, *** FB-MB-DWIBS vs. RT-MB-DWIBS. Each circle represents 1 Likert point.

A: Average whole-body scores for image quality with 95 % confidence intervals. Modified Likert scale: 1 (unacceptable), 2 (poor), 3 (satisfactory), 4 (good) or 5 (excellent).

B: Average whole-body scores for artefacts with 95 % confidence intervals. Modified Likert scale for artefacts from 1 (high impact) to 5 (no impact).

values 0.75–1.0). No significant difference in prostate delineation (p-values 0.50–1.0) was seen.

The overall linear weighted interobserver agreement for subjective image quality incl. ranking was moderate (kappa = 0.53).

3.5. FB-DWIBS vs. RT-MB-DWIBS (**)

In the thorax, RT-MB-DWIBS was rated significantly higher than FB-DWIBS in overall region quality ($p < 0.001$), detection of lymph nodes ($p < 0.05$) and contrast of mediastinum vs. lung ($p < 0.001$). There was no significant difference in overall region sharpness ($p = 0.064$).

In the abdomen, RT-MB-DWIBS was rated significantly higher than FB-DWIBS in overall region quality ($p < 0.001$), overall region sharpness ($p < 0.001$), detection of lymph nodes ($p < 0.001$), spleen homogeneity ($p < 0.05$) and liver delineation ($p < 0.05$).

In the pelvis, no significant differences were observed between FB-DWIBS and RT-MB-DWIBS (p-values 0.19–1.0).

3.6. FB-MB-DWIBS (*,***)

FB-MB-DWIBS was rated significantly lower than both FB-DWIBS and RT-MB-DWIBS for most image parameters in all three stations (overall region quality, overall region sharpness, detection of lymph nodes, liver delineation and spleen homogeneity) (all $p < 0.001$). For contrast of mediastinum vs. lungs, FB-MB-DWIBS scored significantly higher than FB-DWIBS ($p < 0.001$), but significantly lower than RT-MB-DWIBS ($p < 0.001$). Despite being scored significantly lowest in most parameters, FB-MB-DWIBS was not scored less than 3 “satisfactory”.

4. Discussion

The focus of this study was to investigate the artefacts and image quality of the b = 800 s/mm^2 images from DWIBS sequences employing different MB acceleration strategies. The main finding was that using respiratory trigger and MB in DWIBS resulted in improved image quality in areas with respiratory motion: In the thorax and abdomen, respiratory trigger improved the images in approx. half of the rated parameters. However, in the pelvis (where respiratory motion is limited), the use of respiratory trigger did not improve image quality.

Although only very few artefacts were encountered in this study, the MB sequences seemed to induce more artefacts. One reason could be that the separation of slices in MB sequences depends on differences in coil sensitivities and induced phase shifts and temporal disparity between the calibration scan and image acquisition can result in residual aliasing called “slice leakage” [7].

When MB was used only to reduce acquisition time, the results generally showed that FB-MB-DWIBS was rated significantly lower than both FB-DWIBS and RT-MB-DWIBS. However, FB-MB-DWIBS was scanned in half the acquisition time and was still scored “satisfactory” or higher.

The subjective rating of medulla is a marker for a sufficient contrast-to-noise ratio between tissue with restricted diffusion and surrounding normal tissue of the area. In this study, medulla was rated “excellent” in all three sequences. The measurement of SNR in a single volunteer showed similar SNR in low-intensity, non-moving tissues, however the SNR in high-intensity, respiratory-prone tissue was slightly lower in FB-DWIBS than the other sequences.

To our knowledge, no other study has investigated different breathing schemes in whole-body DWI with MB using IR fat saturation (DWIBS).

Other studies have investigated different breathing schemes in combination with SMS or MB in DWI. They all studied organ-specific regions and employed the use of SPAIR fat saturation instead of IR fat saturation. In general, these other studies showed that respiratory-triggered DWI with SMS or MB produced the same or better image quality than free-breathing standard DWI [9,12,17–19]. However, as the techniques behind SMS with SPAIR and MB with IR fat saturation differ slightly, the results, especially at different field strengths, may not be readily interchangeable.

A few studies have investigated MB or SMS in free-breathing whole-body DWI: Buus et al. [24] found that MB reduced acquisition time for free-breathing whole-body DWIBS by 48 % while maintaining a similar subjective image quality at 1.5 T in breast cancer patients.

Taron et al. [11] investigated DWI with SMS on a 3 T PET/MRI system (whole-body, 5–6 stations, SPAIR) and found that in oncological patients, SMS produced lower image quality and more artefacts. Kenkel et al. [14] performed whole-body DWI with SMS and SPAIR at 3 T after failure to produce sufficient image quality with IR fat saturation. They found acquisition time to be reduced by 29 % without significant differences in image quality.

The acquisition time of respiratory triggered sequences will always be dependent on respiratory frequency. In lieu of the fast overall scan time per station, it could be feasible to instruct patients to make shallow and fast breathing as soon as the scanning pauses at the end of each respiratory cycle to minimize acquisition time. Initial pilot experiments indicates that with the short effective scan time of 1.8 s/respiratory cycle, this can be achieved comfortably for the patient over the entire

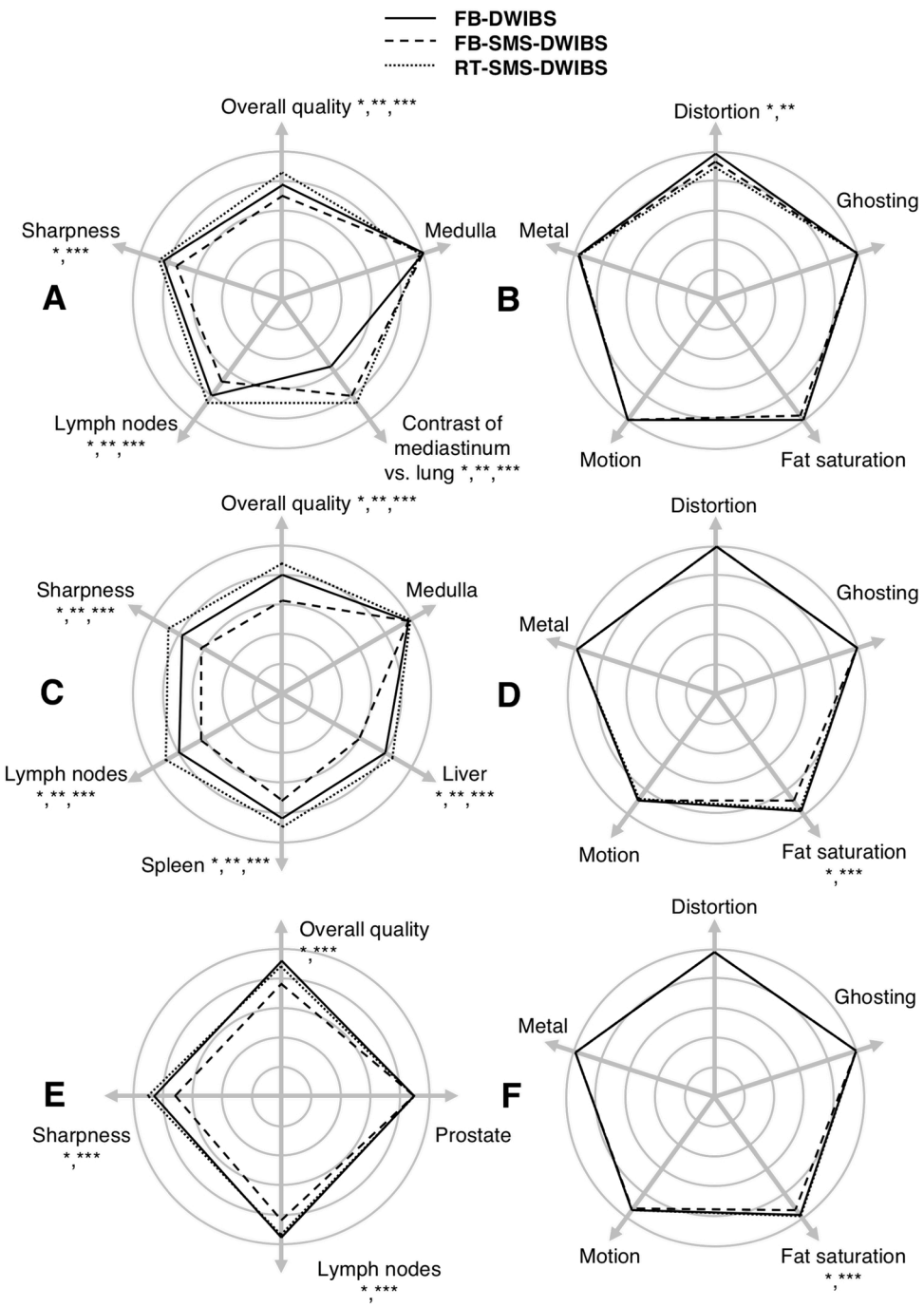

Fig. 3. Subjective image quality and artefacts. A p-value < 0.05 was considered statistically significant: * FB-DWIBS vs. FB-MB-DWIBS, ** FB-DWIBS vs. RT-MB-DWIBS, *** FB-MB-DWIBS vs. RT-MB-DWIBS. Each circle represents 1 Likert point.
A (thorax), B (abdomen) and C (pelvis): Station-wise scores for image quality with 95 % confidence intervals. Modified Likert scale: 1 (unacceptable), 2 (poor), 3 (satisfactory), 4 (good) or 5 (excellent).
D (thorax), E (abdomen) and F (pelvis): Station-wise scores for artefacts with 95 % confidence intervals. Modified Likert scale from 1 (high impact) to 5 (no impact).

length of the scan, but further research is needed.

We did not investigate the variation of ADC, but Larsen et al. [25] found that free-breathing and respiratory compensation produced fairly identical ADC-values in standard DWI. In addition, Buus et al. [24] found that ADC-values were similar in DWIBS with and without MB.

Several authors [1,13] suggest using a fast DWI protocol, e.g., DWIBS or DWI with SMS or MB, as a low-resolution screening tool to rule out malignancy. Our study indicates that FB-MB-DWIBS has the potential to be used as such with satisfactory image quality and an acquisition time of little more than 1 min per station. But further clinical studies in relevant patient populations are needed.

4.1. Limitations

The definitions of the modified Likert scale were quite arbitrary. As a result, the rather similar b = 800 s/mm^2 images from the three sequences in the present study were generally rated 3 (satisfactory) or higher; thus, only the upper end of the Likert scale was employed.

Likert 5 (excellent) was defined as the best possible quality for whole-body DWIBS. It is possible to produce better DWI images, but this would require longer acquisition times or using spectral fat saturation instead of IR fat saturation.

Our patients, who were previously treated for testicular cancer, were relatively young, well-cooperating and motivated for participation. No pathology was observed in the 30 scans. Thus, we were unable to evaluate the diagnostic accuracy of the three sequences. Only 10–20 %

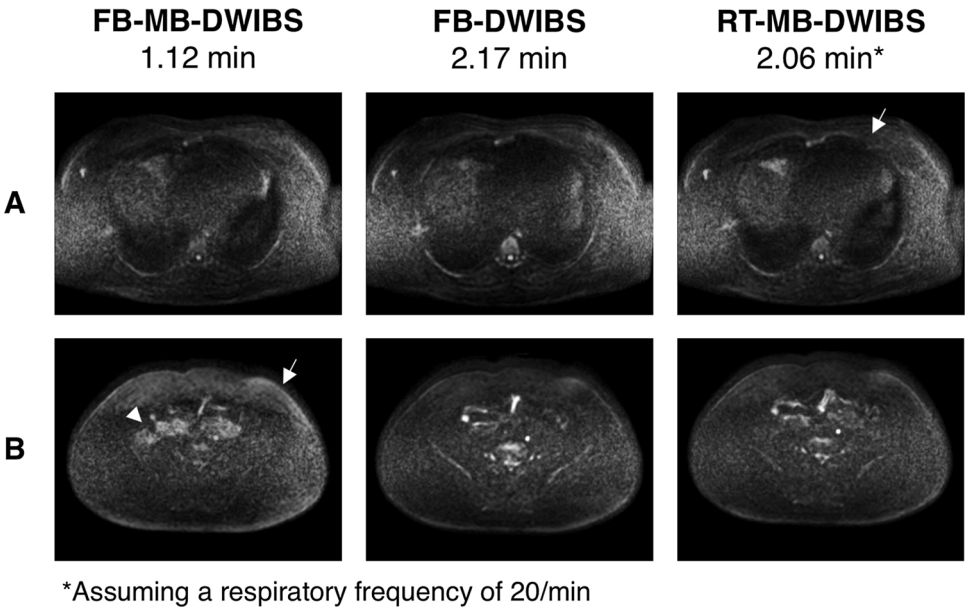

Fig. 4. Image examples of artefacts in corresponding slices of b800 s/mm^2 images from FB-DWIBS, FB-MB-DWIBS and RT-MB-DWIBS:
A: Small distortion artefact on RT-MB-DWIBS in 42-year old male.
B: Fat saturation artefacts on FB-MB-DWIBS in a 27-year old male. In addition, notice the difference in fat saturation in the peritoneal fat.

Table 4
Average ranking scores with 95 % confidence intervals, Friedman test and Wilcoxon signed rank test. Ranked with 1 (worst), 2 (intermediate) or 3 (best). A p-value < 0.05 was considered statistically significant: * FB-DWIBS vs. FB-MB-DWIBS, ** FB-DWIBS vs. RT-MB-DWIBS, *** FB-MB-DWIBS vs. RT-MB-DWIBS.

	Station	FB-DWIBS	FB-MB-DWIBS	RT-MB-DWIBS	Friedman test (k3, n60)		Wilcoxon signed rank test P-value		
					Ft	Ft	*	**	***
Ranking	Thorax	2.0 (1.9−2.1)	1.2 (1.1−1.3)	2.8 (2.7−2.9)	78.43	< 0.001	< 0.001	< 0.001	< 0.001
	Abdomen	2.1 (2.0−2.2)	1.1 (1.0−1.2)	2.8 (2.6−2.9)	80.93	< 0.001	< 0.001	< 0.001	< 0.001
	Pelvis	2.5 (2.4−2.6)	1.1 (1.0−1.2)	2.4 (2.3−2.6)	78.02	< 0.001	< 0.001	0.57	< 0.001
	Average	2.2 (2.1−2.3)	1.1 (1.0−2.3)	2.7 (2.6−2.8)	74.19	< 0.001	< 0.001	< 0.001	< 0.001

Table 5
Subjective image quality with 95 % confidence intervals, Friedman test and Wilcoxon signed rank test. Modified Likert scale: 1 (unacceptable), 2 (poor), 3 (satisfactory), 4 (good) or 5 (excellent). A p-value < 0.05 was considered statistically significant: * FB-DWIBS vs. FB-MB-DWIBS, ** FB-DWIBS vs. RT-MB-DWIBS, *** FB-MB-DWIBS vs. RT-MB-DWIBS.

	Station	FB-DWIBS	FB-MB-DWIBS	RT-MB-DWIBS	Friedman test (k3, n60)		Wilcoxon signed rank test P-value		
					Ft	p-value	*	**	***
Overall region quality	Thorax	3.9 (3.7−4.0)	3.5 (3.4−3.7)	4.3 (4.1−4.4)	32.56	< 0.001	< 0.001	< 0.001	< 0.001
	Abdomen	4.0 (3. 8−4.1)	3.1 (2.9−3.2)	4.4 (4.2−4.6)	71.10	< 0.001	< 0.001	< 0.001	< 0.001
	Pelvis	4.6 (4.4−4.7)	3.8 (3.7−4.0)	4.4 (4.3−4.6)	35.23	< 0.001	< 0.001	0.19	< 0.001
	Average	4.1 (4.0−4.2)	3.5 (3.4−3.6)	4.4 (4.2−4.5)	74.63	< 0.001	< 0.001	< 0.001	< 0.001
Overall region sharpness	Thorax	4.2 (4.0−4.3)	3.7 (3.5−3.8)	4.3 (4.1−4.5)	26.61	< 0.001	< 0.001	0.064	< 0.001
	Abdomen	3.9 (3.8−4.1)	3.1 (3.0−3.3)	4.4 (4.3−4.7)	73.11	< 0.001	< 0.001	< 0.001	< 0.001
	Pelvis	4.3 (4.2−4.5)	3.6 (3.4−3.7)	4.5 (4.3−4.6)	45.26	< 0.001	< 0.001	0.19	< 0.001
	Average	4.1 (4.0−4.3)	3.4 (3.3−3.6)	4.4 (4.3−4.6)	76.76	< 0.001	< 0.001	< 0.001	< 0.001
Detection of lymph nodes	Thorax	4.0 (3.8−4.1)	3.4 (3.2−3.5)	4.3 (4.1−4.5)	39.01	< 0.001	< 0.001	< 0.05	< 0.001
	Abdomen	4.0 (3.8−4.1)	3.1 (2.9−3.3)	4.5 (4.3−4.7)	74.61	< 0.001	< 0.001	< 0.001	< 0.001
	Pelvis	4.8 (4.4−4.9)	4.2 (4.0−4.4)	4.7 (4.6−4.9)	19.60	< 0.001	< 0.001	1.0	< 0.001
	Average	4.2 (4.1−4.3)	3.6 (3.4−3.7)	4.5 (4.4−4.6)	73.51	< 0.001	< 0.001	< 0.001	< 0.001
Medulla	Thorax	5.0 (4.9−5.0)	5.0 (4.9−5.0)	4.9 (4.9−5.0)	0.02	0.99	1.0	0.75	1.0
	Abdomen	4.9 (4.9−5.0)	4.9 (4.9−5.0)	5.0 (4.9−5.0)	0.02	0.99	1.0	1.0	1.0
	Average	5.0 (4.9−5.0)	5.0 (4.9−5.0)	4.9 (4.9−5.0)	0.00	1.00	1.0	1.0	1.0
Contrast of mediastinum vs. lung	Thorax	2.8 (2.6–2.9)	4.0 (3.8−4.2)	4.3 (4.1−4.4)	70.66	< 0.001	< 0.001	< 0.001	< 0.001
Liver delineation	Abdomen	4.0 (3.8−4.2)	3.0 (2.8−3.1)	4.3 (4.0−4.5)	66.66	< 0.001	< 0.001	< 0.05	< 0.001
Spleen homogeneity	Abdomen	4.2 (4.0−4.4)	3.6 (3.3−3.8)	4.5 (4.3−4.7)	32.61	< 0.001	< 0.001	< 0.05	< 0.001
Prostate	Pelvis	4.5 (4.4−4.6)	4.5 (4.3−4.6)	4.5 (4.4−4.6)	0.10	0.95	0.50	1.0	0.50

of patients with stage I testicular cancer experience relapse and in most of these cases the tumor burden is limited [20]. Given this low recurrence rate, thousands of patients would be required to demonstrate a possible difference in diagnostic accuracy or demonstrate non-inferiority.

Therefore, additional research performed in suitable patient groups is needed to investigate the diagnostic performance of whole-body DWIBS in combination with MB. We have initiated a prospective study

of the same three DWIBS sequences in patients with newly diagnosed disseminated testicular cancer.

5. Conclusion

In conclusion, this study shows that although the images produced by FB-DWIBS, FB-MB-DWIBS and RT-MB-DWIBS were very similar, small differences existed. MB enables the use of respiratory trigger while maintaining low acquisition time. Alternatively, MB can be used in very fast DWI sequences that still produce acceptable, although slightly lower, image quality. Future diagnostic studies in relevant patient groups comparing diagnostic performance of FB-MB-DWIBS and RT-MB-DWIBS to standard FB-DWIBS should be performed.

Standards of reporting

The study approach was in accordance with the SQUIRE 2.0 guidelines from the EQUATOR Network [26].

Financial statement/Funding sources

This study was supported by Aarhus University, Aarhus University Hospital and the Health Research Foundation of the Central Denmark Region.

Ethical statements

All procedures performed were in accordance with the ethical standards of the local ethics committee and with the 1964 Declaration of Helsinki and its later amendments or comparable ethical standards. The project was categorized as method development by the local ethics committee which waived the need for written informed consent. Despite this, all patients gave oral consent to additional MRI sequences being scanned and stored in anonymous form.

CRediT authorship contribution statement

Solveig Kärk Abildtrup Larsen: Conceptualization, Methodology, Data curation, Formal analysis, Writing - original draft, Writing - review & editing. **Kim Sivesgaard:** Investigation, Writing - review & editing. **Erik Morre Pedersen:** Conceptualization, Methodology, Investigation, Supervision, Writing - review & editing.

Declaration of Competing Interest

The authors declare that they have no known competing financial interests or personal relationships that could have appeared to influence the work reported in this paper.

Acknowledgements

MRI technician Olga Vendelbo is acknowledged for technical support.

References

[1] T. Takahara, Y. Imai, T. Yamashita, S. Yasuda, S. Nasu, M. Van Cauteren, Diffusion weighted whole body imaging with background body signal suppression (DWIBS): technical improvement using free breathing, STIR and high resolution 3D display, Radiat. Med. 22 (2004) 275–282.

[2] D.-M. Koh, T. Takahara, Y. Imai, D.J. Collins, Practical aspects of assessing tumors using clinical diffusion-weighted imaging in the body, Magn. Reson. Med. Sci. 6 (2007) 211–224, https://doi.org/10.2463/mrms.6.211.

[3] L. Nogueira, S. Brandão, R.G. Nunes, H.A. Ferreira, J. Loureiro, I. Ramos, Breast DWI at 3 T: influence of the fat-suppression technique on image quality and diagnostic performance, Clin. Radiol. 70 (2015) 286–294, https://doi.org/10.1016/j.crad.2014.11.012.

[4] N. Tunariu, M. Blackledge, C. Messiou, G. Petralia, A. Padhani, S. Curcean, A. Curcean, D.-M. Koh, What's new for clinical whole-body MRI (WB-MRI) in the 21st century, Br. J. Radiol. (2020), 20200562, https://doi.org/10.1259/bjr.20200562.

[5] B. Gückel, S. Gatidis, P. Enck, J. Schäfer, S. Bisdas, C. Pfannenberg, N. Schwenzer, Patient comfort during positron emission tomography/magnetic resonance and positron emission tomography/computed tomography examinations: subjective assessments with visual analog scales, Invest. Radiol. 50 (2015) 726–732, https://doi.org/10.1097/RLI.0000000000000177.

[6] V.M. Runge, J.K. Richter, J.T. Heverhagen, Speed in clinical magnetic resonance, Invest. Radiol. 52 (2017) 1–17, https://doi.org/10.1097/RLI.0000000000000330.

[7] M. Barth, F. Breuer, P.J. Koopmans, D.G. Norris, B.A. Poser, Simultaneous multislice (SMS) imaging techniques, Magn. Reson. Med. 75 (2016) 63–81, https://doi.org/10.1002/mrm.25897.

[8] S. Ohlmeyer, F.B. Laun, T. Palm, R. Janka, E. Weiland, M. Uder, E. Wenkel, Simultaneous multislice echo planar imaging for accelerated diffusion-weighted imaging of malignant and benign breast lesions, Invest. Radiol. 54 (2019) 524–530, https://doi.org/10.1097/RLI.0000000000000560.

[9] J. Szklaruk, J.B. Son, W. Wei, P. Bhosale, S. Javadi, J. Ma, Comparison of free breathing and respiratory triggered diffusion-weighted imaging sequences for liver imaging, World J. Radiol. 11 (2019) 134–143, https://doi.org/10.4329/wjr.v11.i11.134.

[10] C.C. Obele, C. Glielmi, J. Ream, A. Doshi, N. Campbell, H.C. Zhang, J. Babb, H. Bhat, H. Chandarana, Simultaneous multislice accelerated free-breathing diffusion-weighted imaging of the liver at 3T, Abdom. Imaging 40 (2015) 2323–2330, https://doi.org/10.1007/s00261-015-0447-3.

[11] J. Taron, C. Schraml, C. Pfannenberg, M. Reimold, N. Schwenzer, K. Nikolaou, P. Martirosian, F. Seith, Simultaneous multislice diffusion-weighted imaging in whole-body positron emission tomography/magnetic resonance imaging for multiparametric examination in oncological patients, Eur. Radiol. 28 (2018) 3372–3383, https://doi.org/10.1007/s00330-017-5216-y.

[12] Y. Pei, S. Xie, W. Li, X. Peng, Q. Qin, Q. Ye, M. Li, J. Hu, J. Hou, G. Li, S. Hu, Evaluation of simultaneous-multislice diffusion-weighted imaging of liver at 3.0 T with different breathing schemes, Abdom. Radiol. (NY) 45 (2020) 3716–3729, https://doi.org/10.1007/s00261-020-02538-y.

[13] E. Weiss, E. Martirosian, E. Notohamiprodjo, E. Kaufmann, E. Othman, E. Grosse, E. Nikolaou, E. Gatidis, Implementation of a 5-minute magnetic resonance imaging screening protocol for prostate cancer in men with elevated prostate-specific antigen before biopsy, Invest. Radiol. 53 (2018) 186–190, https://doi.org/10.1097/RLI.0000000000000427.

[14] D. Kenkel, M.C. Wurnig, L. Filli, E.J. Ulbrich, V.M. Runge, T. Beck, A. Boss, Whole-body diffusion imaging applying simultaneous multi-slice excitation, RoFo Fortschritte Auf Dem Gebiet Der Rontgenstrahlen Und Der Bildgebenden Verfahren 188 (2016) 381–388, https://doi.org/10.1055/s-0035-1567032.

[15] D.-M. Koh, D.J. Collins, Diffusion-weighted MRI in the body: applications and challenges in oncology, AJR Am. J. Roentgenol. 188 (2007) 1622–1635, https://doi.org/10.2214/AJR.06.1403.

[16] A.C. Guyton, J.E. Hall, Textbook of Medical Physiology, 11th ed., Elsevier Saunders, Philadelphia, USA, 2006.

[17] A. Tavakoli, U.I. Attenberger, J. Budjan, A. Stemmer, D. Nickel, S. Kannengiesser, J.N. Morelli, S.O. Schoenberg, P. Riffel, Improved liver diffusion-weighted imaging at 3 T using respiratory triggering in combination with simultaneous multislice acceleration, Invest. Radiol. 54 (2019) 744–751, https://doi.org/10.1097/RLI.0000000000000594.

[18] A. Tavakoli, J. Krammer, U.i.I. Attenberger, J. Budjan, A. Stemmer, D. Nickel, S. Kannengiesser, J.N. Morelli, S.O. Schoenberg, P. Riffel, Simultaneous multislice diffusion-weighted imaging of the kidneys at 3 T, Invest. Radiol. 55 (2020) 233–238, https://doi.org/10.1097/RLI.0000000000000637.

[19] J. Taron, P. Martirosian, M. Erb, T. Kuestner, N.F. Schwenzer, H. Schmidt, V. S. Honndorf, J. Weiβ, M. Notohamiprodjo, K. Nikolaou, C. Schraml, Simultaneous multislice diffusion-weighted MRI of the liver: analysis of different breathing schemes in comparison to standard sequences, J. Magn. Reson. Imaging 44 (2016) 865–879, https://doi.org/10.1002/jmri.25204.

[20] M.P. Laguna, P. Albers, F. Algaba, C. Bokemeyer, J.L. Boormans, S. Fischer, K. Fizazi, H. Gremmels, R. Leão, D. Nicol, N. Nicolai, J. Oldenburg, T. Tandstad, J. Mayor De Castro, C.D. Fankhauser, F. Janisch, T. Muilwijk, Y. Jain, EAU guidelines on testicular cancer Edn, in: Presented at the EAU Annual Congress Amsterdam 2020, Arnhem, The Netherlands, 2020.

[21] S.B. Reeder, Measurement of signal-to-noise ratio and parallel imaging, in: S. O. Schoenberg, O. Dietrich, M.F. Reiser (Eds.), Parallel Imaging in Clinical MR Applications, Springer Berlin Heidelberg, Berlin, Heidelberg, 2007, pp. 49–61, https://doi.org/10.1007/978-3-540-68879-2_4.

[22] G. Norman, Likert scales, levels of measurement and the "laws" of statistics. (Report), Adv. Health Sci. Educ. 15 (2010) 625–632, https://doi.org/10.1007/s10459-010-9222-y.

[23] J.R. Landis, G.G. Koch, The measurement of observer agreement for categorical data, Biometrics 33 (1977) 159–174, https://doi.org/10.2307/2529310.

[24] T.W. Buus, K. Sivesgaard, A.B. Jensen, E.M. Pedersen, Simultaneous multislice diffusion-weighted imaging with short tau inversion recovery fat suppression in bone-metastasizing breast cancer, Eur. J. Radiol. 130 (2020), 109142, https://doi.org/10.1016/j.ejrad.2020.109142.

[25] N.E. Larsen, S. Haack, L.P.S. Larsen, E.M. Pedersen, Quantitative liver ADC measurements using diffusion-weighted MRI at 3 Tesla: evaluation of reproducibility and perfusion dependence using different techniques for respiratory compensation, Magma (New York, N.Y.) 26 (2013) 431–442, https://doi.org/10.1007/s10334-013-0375-6.

[26] G. Ogrinc, L. Davies, D. Goodman, P. Batalden, F. Davidoff, D. Stevens, SQUIRE 2.0 (Standards for QUality Improvement Reporting Excellence): revised publication

guidelines from a detailed consensus process, BMJ Qual. Saf. 25 (2016) 986–992, https://doi.org/10.1136/bmjqs-2015-004411.